# WIND-INDUCED RESPONSE OF TORSIONALLY COUPLED HIGH-RISE BUILDINGS INCLUDING SOIL FLEXIBILITY

**EL-Sayed Amin Mashaly**
Structural Engineering Department, Faculty of Engineering
Alexandria University, Alexandria, Egypt

ABSTRACT

A general formulation of the problem of lateral-torsional dynamic response of tall buildings to stochastic wind loads is presented including the dynamic soil-structure interaction. The wind forcing functions are treated as multiple random processes characterized by spectra and co-spectra in along wind, across wind, and torsional directions at different floor levels. The building is modelled as a shear frame on a rectangular rigid footing attached to the surface of a linearly elastic half space. The soil-structure interaction of the footing is represented by impedance functions which are expressed by empirical formulas. A random vibration based procedure is used to estimate the response statistics that are important for checking the serviceability of the building. A wide parametric study has been carried out in order to investigate the effect of soil flexibility, structural properties, and torsional coupling of asymmetric buildings. The results of this study indicate that:(i) the significance of torsional and across wind responses suggests that the criteria limiting the maximum drift and acceleration of high-rise building as a serviceability limit state must address the lateral torsional motion and soil flexibility, and (ii) wind induced responses increase significantly with the height;this effect is pronounced for flexible buildings.

*Keywords: Structural analysis, Wind engineering, High-rise buildings*

INTRODUCTION

The lateral strength of the buildings in areas other than the high seismic zones is mainly governed by wind-induced vibration. This aspect is more evident in zones of severe wind and for tall or long structures. The tendency towards the construction of tall slender and flexible buildings has forced designers to recognize the unsteady nature of wind loading and to modify their designs to ensure satisfactory performance of the buildings under these unsteady loads. Under the influence of dynamic wind loads, the high rise buildings oscillate in along wind, across wind, and torsional directions. The along wind force results primarily from pressure fluctuations on the windward and leeward which follow the fluctuations in the approach flow, at least in the low frequency range. The across wind force arises from nonhomogeneous pressure fluctuations in the separated shear flow and wake flow fields adjacent to the side faces. The wind-induced torsional moments result from the unbalance in the instantaneous pressure distribution on the building surface. The wind loads effects are further amplified in asymmetric building as a result of inertial coupling. Design procedures that treat the dynamic response of high-rise buildings to wind focus on the along wind response of such buildings induced by buffeting from incident turbulence [1-8]. However, the across wind forces and torsional moments are known to be the major factors in causing objectionable building motion [9-11]. The design of tall buildings should be controlled not only by the strength (which depends on wind induced stresses) but also by the serviceability requirements and in particular by the need to limit the building deformations in the upper floors to an acceptable level for human comfort.

The along wind response has been shown to be satisfactory treated by a gust factor approach. Random vibration-based gust load and response factors developed by Davenport [1], Vellozi, and

Cohen [2] translated the dynamic loading caused by unsteady wind into an equivalent static loading producing the same deflections and stresses. They modelled the building as a SDOF system assuming a straight line first vibration mode shape. Solari [3] developed two expressions for the power spectrum and coherence function of along wind fluctuations. Solari [4, 5] introduced an equivalent wind spectrum model in which the wind is schematized as a stochastic stationary Gaussian process made up of a mean velocity profile on which an equivalent turbulent fluctuation defined by the reduced equivalent wind spectrum is superimposed. This model was then employed for defining the along wind structural response spectrum. Furthermore, Solari [6] presented a general expression of the power spectrum of along wind turbulence for calculating the equivalent pressure on the structures and their responses. Li and Kareem [7] used the recursive modelling for analyzing the structural response to correlated multi input loading due to fluctuations in along wind direction. Chen, and Ahmadi [8] used the method of equivalent linearization for the response analysis of base-isolated structure in the along wind direction to the fluctuating part of wind velocity.

The complex nature of wake-excited across wind and torsional responses which result from the nonlinear interaction of incident turbulence, wake dynamics, and building motion has inhibited analytical prediction of aerodynamic loads in terms of gust factors. Instead, semi-analytical methods have been developed for predicting the across wind and torsional loading functions relying on spatio temporal measurements of the fluctuating pressure field around aeroelastic model in wind tunnel tests. Kareem et al [12] developed expressions for across wind forcing functions in time and frequency domains based on statistical integration;those functions are then used for estimating the dynamic response of tall buildings. Kwok and Melbourne [13] studied the across wind response of structures due to displacement lock-in excitation. Tsukagoshi et al [14] conducted response analyses on along wind and across wind vibrations of a tall building in time domain using a numerical simulation technique. Sidarous and Vanderbilt [15] presented a methodology for predicting the dynamic response levels of building under wind loading, that consists of the along wind, across wind forces, and the torsional moments. Kareem [9,16] presented expressions for the spectra of along wind, across wind forces and torsional moments which were used for the stochastic response analysis of a special class of torsionally coupled building(in which the centers of masses of all floors lie on one vertical axis and all stories have the same radius of gyration and same ratios of translational and torsional stiffnesses). Islam et al [10, 11] obtained the generalized spectra of the along wind, across wind, and torsional components of wind forces and the correlation among them, using a time series analysis of surface pressure measured during wind tunnel test around a rigid model. These spectra were used through stochastic analysis for calculating the accelerations at the top of symmetrical buildings and a special class of asymmetrical buildings.

The previous studies on wind induced response of tall building has been focused on the evaluation of the displacements and accelerations of the top floors from the point of view of building serviceability. Only, the fundamental mode associated with each direction of motion was considered in the modal analysis. Moreover, the procedures developed in the literature for calculating the structural response to forces induced by atmospheric turbulence are based on the assumption that the structure is modelled as a linear cantilever with fixed base. However, this assumption may be unrealistic for heavy structures on a deep soft soil. In such cases, the soil flexibility produces two opposite effects on the structural response, (i) amplification due to the modifications of the natural frequencies and the rigid body motion of the base, and (ii) deamplification due to the damping of soft soil. Solari and Stura [17] presented a simplified formulation of the problem of the dynamic along wind response of a structural system including the soil flexibility using the classical modal analysis. But, the soil-foundation-structure system does not posses classical normal modes and the normal mode superposition is not rigorously applicable to the study of such a system. Therefore, the nonclassical modal analysis, or the direct frequency method have to be used for evaluating the response parameters to ensure a viable and economical structural system.

In this paper, a comprehensive procedure for calculating the dynamic response of torsionally coupled tall building to wind induced excitation is proposed. The wind loading is represented by the three components in along wind, across wind, and torsional directions which are characterized by spectra and cross spectra at different floor levels. The building is modelled as a shear frame on a rectangular rigid footing attached to the surface of a linearly elastic half space. The dynamic d. o. f of the soil-foundation-structure system consist of two horizontal translations and twisting about the vertical axis for each floor, as well as five base d. o. f. The soil-structure interaction for the footing is represented by impendance functions expressed by empirical formulas representing both the stiffness and damping of soil. A stochastic analysis is conducted in the frequency domain to estimate the root mean square (r.m.s) and peak values of displacements, accelerations, base shears, and base moments.

## QUANTIFICATION OF WIND LOADING

It follows from the nature of wind that a structure exposed to wind will experience a steady load associated with the mean wind and fluctuating forces associated principally with the gusts. The latter can be resolved into along wind forces acting in the direction of the wind flow and across wind forces acting perpendicular to it. The resultant wind forces seldom coincides with the stiffness and/or mass centres of the structure. As a result the building is subjected to torsional moments.

### *Along Wind (or Drag) Forces*

The along wind forces can be treated successifuly using classical theories of fluid mechanics [1, 2]. The instantaneous wind velocity $V_z(t)$ at a height Z is defined as

$$V_z(t) = \bar{V}_z + v_z(t) \quad (1)$$

where $\bar{V}_z$ is the mean wind velocity, and $v_z(t)$ is the longitudinal component of turbulence (velocity fluctuation) which is usually treated as stochastic stationary Gaussian process with zero mean characterized by a power spectral density function (PSDF), $S_v(n)$. Many forms for $S_v(n)$ are available in the literature [1-6, 8, 14, 15]; they have been obtained using extensive series of experimental tests on aeroelastic models in wind tunnels. The PSDF given by Solari [3, 6] is used herein to obtain that for the ith floor at height $Z_i$ as

$$\frac{nS_{v_i}(n)}{U_*^2} = \frac{2.21\beta^{2.5}f_i}{(1+3.31\beta^{1.5}f_i)^{5/3}} \quad (2)$$

in which n=frequency (Hz), ($n=\omega/2\pi$), $U_*$=shear velocity that is obtained as

$$U^2_* = \sigma_v^2/\beta \quad (3a)$$

where $\sigma^2_v$=variance of the longitudinal component of velocity fluctuation, $\beta$=nondimensional function given as

$$\beta = 4.5 - 0.856 \ln Z_0 \quad (3b)$$

$Z_0$ = surface roughness height ($.03<Z_0<1.0$m), $f_i$=Monin's coordinate given as

$$f_i = \frac{nZ_i}{\bar{V}_{z_i}} \quad (3c)$$

and $\bar{V}_{zi}$ is the mean wind velocity at height $Z_i$ that is calculated as

$$\bar{V}_{z_i} = 2.5U_* \ln(Z_i/Z_0) \quad (3d)$$

To relate the along wind load spectrum to the velocity spectrum, it is assumed that at a given height Z, the wind load $F_z(t)$ is proportional to the square of velocity $V_z(t)$,

$$F_z(t) = \frac{1}{2}\rho_a C_d A V_z^2(t) = CV_z^2(t) \quad (4)$$

where $\rho_a$=air density, $C_d$=drag coefficient, A=frontal area of building. Since v(t) is small, then from Eqs. 1 and 4, $F_z(t)$ is written as

$$F_z(t) \approx C(\bar{V}_z^2 + 2\bar{V}_z v(t)) \approx C\bar{V}_z^2\left(1+\frac{2v(t)}{\bar{V}_z}\right) \approx \bar{F}_z\left(1+\frac{2v(t)}{\bar{V}_z}\right) \quad (5)$$

also, following Eq. 1, $F_z(t)$ can be rewritten as

$$F_z(t)=\bar{F}_z+f(t) \qquad (6)$$

where $\bar{F}_z$, f(t) are the mean and fluctuating components of the load. From Eqs. 5 and 6, f(t) is given as function of v(t) as

$$f(t)=\frac{2\bar{F}_z}{\bar{V}_z}v(t) \qquad (7)$$

The PSDF, $S_{fi}(n)$ of the along wind force $f_i(t)$ at height $Z_i$, can be obtained using Eq. 7 and the principles of spectral analysis as

$$S_{f_i}(n)=\frac{4\bar{F}^2_{z_i}}{\bar{V}^2_{z_i}}S_{v_i}(n) \qquad (8)$$

Now, an aerodynamic admittance function $L_i(n)$ is introduced in Eq. 8 to account for the spatial characteristics of the turbulence, their organization over the body, and aerodynamic efficiency of the building in generating force. i. e Eq. 8 becomes

$$S_{f_i}(n)=\frac{4\bar{F}^2_{z_i}}{\bar{V}^2_{z_i}}S_{v_i}(n)L_i(n) \quad , \quad L_i=J_{v_i}(n)*J_{H_i}(n) \qquad (9)$$

where $J_{vi}(n)$, $J_{Hi}(n)$ are the vertical and horizontal aerodynamic admittance functions that are obtained as [7]

$$J_{v_i}=\frac{2}{(\gamma_{z_i}C_z)^2}[\exp(-\gamma_{z_i}C_z)+\gamma_{z_i}C_z-1]$$

$$J_{H_i}=\frac{2}{(\gamma_{y_i}C_y)^2}[\exp(-\gamma_{y_i}C_y)+\gamma_{y_i}C_y-1] \qquad (10)$$

$$\gamma_{y_i}=\frac{2n\sqrt{1+r^2}}{\bar{V}_{o_i}(1+r)}B \ , \ \gamma_{z_i}=\frac{2n\sqrt{1+r^2}}{\bar{V}_{o_i}(1+r)}D_i, r=\frac{C_yB}{C_zD_i}$$

$C_y$ and $C_z$=decay constants, B=building width, $D_i$=height of ith floor, and $V_{oi}$=mean wind velocity at the centroide of ith segment.

The cross PSDF, $S_{fij}(n)$ of the along wind forces $f_i(t)$, $f_j(t)$ at ith and jth floors is given as

$$S_{f_{ij}}(n)=\sqrt{S_{f_i}(n)S_{f_j}(n)Coh_{ij}(n)} \qquad (11)$$

in which $Coh_{ij}(n)$ is a coherence function representing the cross correlation between the components of the turbulence at heights $z_i$, $z_j$. The study in the literature showed that, $Coh_{ij}(n)$ tends to diminish as the separation height $|z_i-z_j|$ and wave number $n/\bar{V}_{\bar{z}}$ increase, i. e

$$Coh_{ij}(n)=\exp(-\frac{nC_z|z_i-z_j|}{\bar{V}_{\bar{z}}}) \ , \bar{V}_{\bar{z}}=\frac{\bar{V}_{z_i}+\bar{V}_{z_j}}{2} \qquad (12)$$

*Across Wind (or Lift) Force and Torsional Moment*

The mechanisms giving rise to across wind and torsional forces have proved to be so complex that analytical formulation of these forces based on the characteristics of the incident turbulence is not possible. The only recourse is the determination of the spectra of these forces directly from the spatio temporal measurements of the fluctuating pressure field around tall building models in the wind tunnel tests. Kareem [9, 16] developed an empirical expression for the spectrum of torsional moment $M_t(t)$ for urban flow condition. This spectrum is reproduced in nondimensional form in Figure (1). Using the formula presented by Tsukagoshi et al [14], the following empirical expression is suggested for the PSDF of across wind force $F_i(t)$,

$$S_{f_i}(n)=\bar{F}^2_{z_i}\frac{\bar{B}}{65\pi n}*\frac{\bar{K}^2}{(1-\bar{K}^2)^2+(2\bar{B}\bar{K})^2}, \bar{K}=nW/\bar{V}_HS \qquad (13)$$

where $\bar{V}_H$ is the mean wind velocity at the top of building and S, $\bar{B}$ are the Strouhal number and band width (respectively) that are given as

$$S=0.135-0.069\exp(-0.056H/W), \bar{B}=0.6\exp(-0.3H/W) \qquad (14)$$

in which H, W are the height and the across wind dimension of the building.

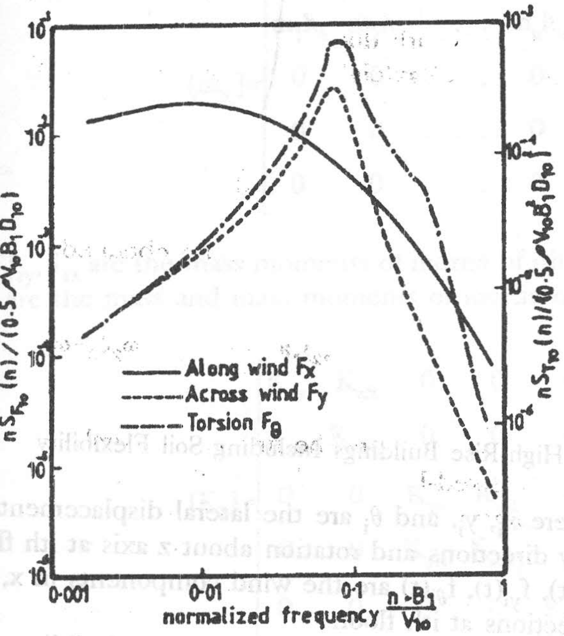


Figure 1. Normalized power spectra of 10th floor wind forces.

The PSDF's of along wind force (represented by Eqs. 2, 3, 9, 10) and across wind force given by Eqs. 13, 14 for the top floor are plotted in a nondimensional form in Figure (1), in which B1 is the square root of the plan area of the building.

The cross PSDF of the across wind forces and torsional moments can be obtained using equations similar to Eq. 11 in which the PSDF $S_{fi}$, $S_{fj}$ are replaced by those of across wind forces and torsional moments, respectively.

## ANALYTICAL FORMULATION

### *Structural Idealization*

The structure-foundation system considered is a linear torsionally coupled multi-storey shear building on flexible foundation shown in Figure (2). The building has n floors connected by weightless columns;the mass centre (CM) and resistance centre (CR) are eccentrically placed in x and y directions by amounts $e_x$ and $e_y$. Thus, the descretized building model in the global coordinate system consists of two lateral translations (in two orthogonal directions x, and y) and twisting (about the vertical axis z) per each storey level. The building footing is idealized as a rigid rectangular plate resting on the surface of a linearly elastic half space;five d.o.f are assigned for the footing, namely two horizontal translations in x, and y directions, two rocking about these directions, and twisting about z axis.

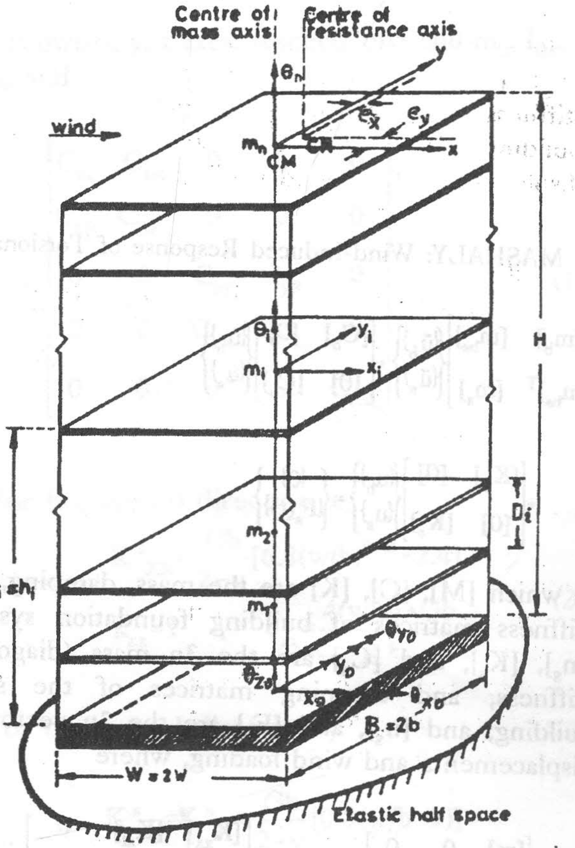


Figure 2. Model of torsionally coupled building with soil-foundation system.

### *Equations of Motion*

The building-foundation system considered (with eccentric centres of mass and resistance) responds in coupled lateral and torsional motion due to the unsteady aerodynamic loads. The governing equations of system motion can be written in a matrix form as

$$[M]\{\ddot{U}\}+[C]\{\dot{U}\}+[K]\{U\}=\{F(t)\} \tag{15}$$

or

$$\begin{bmatrix}[m_b] & [m_{bs}]\\ [m_{bs}]^T & [m_s]\end{bmatrix}\begin{Bmatrix}\{\ddot{u}_b\}\\ \{\ddot{u}_s\}\end{Bmatrix}+\begin{bmatrix}[C_b] & [0]\\ [0] & [C_s]\end{bmatrix}\begin{Bmatrix}\{\dot{u}_b\}\\ \{\dot{u}_s\}\end{Bmatrix} \qquad (16)$$

$$+\begin{bmatrix}[K_b] & [0]\\ [0] & [K_s]\end{bmatrix}\begin{Bmatrix}\{u_b\}\\ \{u_s\}\end{Bmatrix}=\begin{Bmatrix}\{0\}\\ \{F_s(t)\}\end{Bmatrix}$$

in which [M], [C], [K] are the mass, damping, and stiffness matrices of building foundation system; $[m_s]$, $[K_s]$, and $[C_s]$ are the 3n mass (diagonal), stiffness, and damping matrices of the shear building; and $\{u_s\}$, and $\{F_s\}$ are the 3n vectors of displacements and wind loading, where

$$[m_s]=\begin{bmatrix}[m] & 0 & 0\\ 0 & [m] & 0\\ 0 & 0 & [m]\end{bmatrix},\quad [K_s]=\begin{bmatrix}[K_{xx}] & [K_{xt}] & 0\\ [K_{xt}]^T & [K_{tt}] & [K_{yt}]^T\\ 0 & [K_{yt}] & [K_{yy}]\end{bmatrix}, \qquad (17a)$$

$$\{u_s\}=\{(x)\ \ (r\theta)\ \ (y)\}^T,\{F_s(t)\}=\{(f_x(t))\ \ (\frac{1}{r}f_\theta(t))\ \ (f_y(t))\}^T$$

The submatrices [m], $[K_{xx}]$, $[K_{yy}]$, $[K_{tt}]$, $[K_{xt}]$ and $[K_{yt}]$ are defined in terms of the geometric properties of different stories i. e (for ith storey) the lumped mass $m_i$;the lateral stiffnesses $K_{xi}$, $K_{yi}$ in x,y directions; the torsional stiffness $K_{\theta i}$;the eccentricities $e_{xi}$, $e_{yi}$ between mass and resistance centres in x, y directions;and the radius of gyration $r_i$. The sub-vectors are given by

$$(x)=(x_1\ \ x_2\ \ .\ .\ .\ \ x_n)^T,$$
$$(r_\theta)=(r_1\theta_1\ \ r_2\theta_2\ \ .\ .\ .\ \ r_n\theta_n)^T,$$
$$(y)=(y_1\ \ y_2\ \ .\ .\ .\ \ y_n)^T,$$
$$(f_x(t))=(f_{x1}(t)\ \ f_{x2}(t)\ \ .\ .\ \ f_{xn}(t))^T, \qquad (17b)$$

where $x_i$, $y_i$, and $\theta_i$ are the lateral displacements in x, y directions and rotation about z axis at ith floor; $f_{xi}(t)$, $f_{yi}(t)$, $f_{\theta i}(t)$ are the wind components in x, y, $\theta$ directions at ith floor.

Assuming Rayleigh's damping for the building, $[C_s]$ is related to $[m_s]$ and $[K_s]$ as

$$[C_s]=a_0[m_s]+a_1[K_s] \qquad (18a)$$

where the coefficients $a_0$, $a_1$ are obtained as

$$a_0=\frac{2\omega_1\omega_2}{\omega_2^2-\omega_1^2}(\omega_2\zeta_1-\omega_1\zeta_2),\ a_1=\frac{2}{\omega_2^2-\omega_1^2}(\omega_2\zeta_2-\omega_1\zeta_1) \qquad (18b)$$

in which $\omega_1$, $\omega_2$ are the first two natural frequencies of the fixed-base building, and $\zeta_1$, $\zeta_2$ are the modal damping ratios assigned for the first two modes.

Again, in Eq. 16, $\{u_b\}$ is the vector of footing d.o.f; $[m_b]$ is the mass matrix of the footing;and $[m_{bs}]$ is a mass matrix denoting the coupling between the building d.o.f and the footing d.o.f, $[K_b]$, and $[C_b]$ are the stiffness and damping matrices of the footing, where

$$\{u_b\}=\{x_0\ \ \theta_{y_0}\ \ y_0\ \ \theta_{x_0}\ \ \theta_{z_0}\}^T, \qquad (19a)$$

$$[m_b]=\begin{bmatrix}m_t & L_t & 0 & 0 & 0\\ L_t & I_{b_x} & 0 & 0 & 0\\ 0 & 0 & m_t & L_t & 0\\ 0 & 0 & L_t & I_{b_y} & 0\\ 0 & 0 & 0 & 0 & I_{b_z}\end{bmatrix} \qquad (19b)$$

$$m_t=m_0+\sum^n m_i,\ \ L_t=\sum^n m_i h_i,\ I_b=I_0+\sum^n I_i$$

$$[m_{b_s}]=\begin{bmatrix} m_1 & m_2 & \cdots & m_n & 0 & 0 & \cdots & 0 & 0 & 0 & \cdots & 0 \\ m_1h_1 & m_2h_2 & \cdots & m_nh_n & 0 & 0 & \cdots & 0 & 0 & 0 & \cdots & 0 \\ 0 & 0 & \cdots & 0 & 0 & 0 & \cdots & 0 & m_1 & m_2 & \cdots & m_n \\ 0 & 0 & \cdots & 0 & 0 & 0 & \cdots & 0 & m_1h_1 & m_2h_2 & \cdots & m_nh_n \\ 0 & 0 & \cdots & 0 & I_{z_1} & I_{z_2} & \cdots & I_{z_n} & 0 & 0 & \cdots & 0 \end{bmatrix} \tag{19d}$$

$I_{iz}$, $I_{iy}$, $I_{iz}$ are the mass moments of inertia of ith floor about its own x, y, z axes, respectively; and $m_0$, $I_{0x}$, $I_{0y}$, $I_{0z}$ are the mass and mass moments of inertia of the footing, and

$$[K_b]=\begin{bmatrix} K_{xx} & K_{xR} & 0 & 0 & 0 \\ K_{xR} & K_{RR_x} & 0 & 0 & 0 \\ 0 & 0 & K_{yy} & K_{yR} & 0 \\ 0 & 0 & K_{yR} & K_{RR_y} & 0 \\ 0 & 0 & 0 & 0 & K_{RR_z} \end{bmatrix}, \quad [C_b]=\begin{bmatrix} C_{xx} & C_{xR} & 0 & 0 & 0 \\ C_{xR} & C_{RR_x} & 0 & 0 & 0 \\ 0 & 0 & C_{yy} & C_{yR} & 0 \\ 0 & 0 & C_{yR} & C_{RR_y} & 0 \\ 0 & 0 & 0 & 0 & C_{RR_z} \end{bmatrix} \tag{19e}$$

In the above equations, K's, C's are stiffness and damping coefficients representing the real and imaginary parts of soil impedance functions (dynamic stiffness) $K^d$, which are analytically obtained by solving the mixed boundary value problems arising from applying a harmonic force, moment, or torque separately to a footing on an elastic half space. Pais and Kausel [18] proposed approximate formulas for the frequency-dependent dynamic stiffnesses $K^d$'s of a rigid rectangular surface footing of dimensions 2b*2w (b<w), in horizontal, rocking, and torsional directions, where

$$K^d=K^s[k+ia_0c] \tag{20}$$

in which $a_0$ is a dimensionless frequency ($a_0=\omega b/V_s$), $\omega$=frequency of vibration, $V_s$=shear wave velocity of soil ($V_s=\sqrt{G/\rho_s}$), G, $\rho_s$ are the shear modulus and mass density of soil, $K^s$ designates the approximate static stiffness, and k's, c's are stiffness and damping coefficients, where

a-For horizontal direction x

$$K^s_{xx}=\frac{Gb}{2-\nu}[6.8(w/b)^{0.65}+2.4]$$

$$k_{xx}=1 \quad , \quad c_{xx}=\frac{4(w/b)*Gb}{K^s_{xx}} \tag{21a}$$

b-For horizontal direction y

$$K^s_{yy}=K^s_{xx}+\frac{Gb}{2-\nu}[0.8(w/b-1)]$$

$$k_{yy}=1, \quad c_{yy}=\frac{4(w/b)*Gb}{K^s_{yy}} \tag{21b}$$

c-For coupling

$k_{xR}=c_{xR}=0.0$ ,$k_{yR}=c_{yR}=0.0$ (for surface footing), (21c)

d-For rocking, direction x

$$K^s_{RR_x}=\frac{Gb^3}{1-\nu}*[3.2(w/b)+0.8],$$

$$k_{RR_x}=1-\frac{da_0^2}{b+a_0^2}, d=0.55+0.1\sqrt{w/b-1}, b=2.4-\frac{0.4}{(w/b)^3} \tag{21d}$$

$$c_{RR_x}=\frac{4\alpha(w/b)*Gb^3}{3K^s_{RR_x}}*\frac{a_0^2}{f+a_0^2}, f=2.2-\frac{0.4}{(w/b)^3}$$

e-For rocking, direction y

$$K^{s}_{RR_y}=\frac{Gb^3}{1-\nu}*[3.73(w/b)^{2.4}+0.27]$$

$$k_{RR_y}=1-\frac{da_0^2}{b+a_0^2},d=0.55,b=0.6+\frac{1.4}{(w/b)^3} \tag{21e}$$

$$c_{RR_y}=\frac{4\alpha(w/b)^3*Gb^3}{3K^{s}_{RR_y}}*\frac{a_0^2}{f+a_0^2},f=\frac{1.8}{1+1.75(w/b-1)},$$

f-For torsion

$$K^{s}_{RR_z}=Gb^3*[4.25(w/b)^{2.45}+4.06]$$

$$k_{RR_z}=1-\frac{da_0^2}{b+a_0^2},d=0.33-0.03\sqrt{w/b-1},b=\frac{0.8}{1+0.33(w/b-1)}$$

$$c_{RR_z}=\frac{4[(w/b)^3+(w/b)]Gb^3}{3K^{s}_{RR_z}}*\frac{a_0^2}{f+a_0^2},f=\frac{1.4}{1+3(w/b-1)^{0.7}}$$

$$\text{where } \alpha=\sqrt{2(1-\nu)/(1-2\nu)}\ ,\nu=\text{Poisson's ratio} \tag{21f}$$

*Response Analysis*

As mentioned earlier, the soil-structure interaction gives rise to a nonclassically damped system. In such cases, the undamped mode shapes do not uncouple the equations of motion. The modal superposition can be employed for the response analysis using the damped (complex) mode shapes. However, the frequency-dependence of the foundation stiffness and damping matrices leads to nonlinear eigen value problem. To overcome this difficulty, the response is analyzed in frequency domain using the direct frequency method, in which the complex frequency response functions are obtained at any particular excitation frequency(n). The matrices of complex frequency response functions of displacements, velocities, and accelerations are obtained as

$$[H(i2\pi n)]=(2\pi n)^p[-(2\pi n)^2[M]+i2\pi n[c]+[K]]^{-1} \tag{22}$$

with p=0, 1, and 2 for displacements, velocities, and accelerations, respectively. The matrix of complex frequency functions of forces, torsional moments at different floor levels, the base moments, and base shears is obtained using that of displacements, as

$$[Q(i2\pi n)]=[K][H(i2\pi n)] \tag{23}$$

Since the wind loading in Eq. 16 is stochastic in nature, the dynamic response of the building must be obtained using the methods of random vibration. A spectral analysis in frequency domain is utilized in the present study. As mentioned before, the fluctuating wind forces are usually considered as stationary random processes with zero means, and since the system is linear, the structural responses will be also stationary random processes with zero means. The relationship between the forcing functions {F(t)} and the response functions {R(t)} is given by

$$[S_R(n)]=[B(i2\pi n)]^*[S_F(n)][B(i2\pi n)]^T \tag{24}$$

in which $[S_R(n)]$ and $[S_F(n)]$ are the PSDF matrices of the response functions, and the forcing functions, respectively;$[B(i2\pi n)]$is the matrix of complex frequency response functions of the response (which varies and depends upon the response quantity to be evaluated);*, T denote the complex conjugate and transpose, respectively. The fluctuating wind forces in the along wind and across wind directions are generally independent for typical prismatic buildings [16]. Also, in this study, it is assumed that the loads in the lateral and torsional directions are uncorrelated. Consequently, $[S_F(n)]$ becomes

$$[S_F(n)]=\begin{bmatrix}[0] & 0 & 0 & 0\\ 0 & [S_{f_x}(n)] & 0 & 0\\ 0 & 0 & [S_{f_\theta}(n)] & 0\\ 0 & 0 & 0 & [S_{f_y}(n)]\end{bmatrix} \tag{25}$$

where $[S_{Fx}(n)]$, $[S_{fy}(n)]$, $[S_{f\theta}(n)]$ are the submatrices of PSDF functions of along wind, across wind, and torsional loads, respectively. The matrix of mean square responses $[E[R^2(t)]]$(same as that of variances $[\sigma^2_R]$) is given as

$$[\sigma^2_R]=\int_0^\infty[S_R(n)]dn \tag{26}$$

from which the root mean square (r.m.s) values (same as standard deviation $\sigma_R$) may be calculated.

The corners of a building experience considerable effects of torsional response. Therefore, it is important to consider the response at the top of building which for the corner (at $x=W/2$, $y=B/2$) is obtained from the response at the centre of the building mass (CM) as

$$X_c^{p}(t)=x^{p}(t)-\frac{B}{2}\theta^{p}(t),\; y^{p}_c(t)=y^{p}(t)+\frac{W}{2}\theta^{p}(t) \quad (27)$$

in which $x_c(t)$ and $y_c(t)$ are the x and y components of corner response; $x(t)$ and $y(t)$ are the x and y components of centre response and p stands for higher derivatives of response ($p=0$, 2 for displacements and accelerations, respectively). The r. m. s values (or standard deviations) of the building corner responses are given by

$$\sigma_{x_c}=\sqrt{\sigma^2_x+\frac{B^2}{4}\sigma^2_\theta-B\sigma^2_{x_\theta}},\;\sigma_{y_c}=\sqrt{\sigma^2_y+\frac{w^2}{4}\sigma^2_\theta+w\sigma^2_{y_\theta}} \quad (28)$$

The probabilistic description of peak response of a building subjected to random wind excitation can be obtained from theoretical consideration of the probability density of the extreme value of a Gaussian stationary random signal. The mean peak value of response quantity $R_i(t)$ is obtained as

$$\mu_{R_i}=K^*_i\sigma_{R_i} \quad (29)$$

$\sigma_{Ri}$ is the r. m. s value of $R_i(t)$ (Eq. 26) and $K_i^*$ is a peak factor given as

$$K^*_i=\sqrt{2\ln(\nu_{0_i}T)}+0.5772/\sqrt{2\ln(\nu_{0_i}T)} \quad (30)$$

where T is the wind duration in sec., $\nu_0$ is the rate of zero crossing expressed as

$$\nu_{0_i}=\frac{1}{2\pi}\sqrt{\lambda_{2_i}/\lambda_{0_i}} \quad (31)$$

in which $\lambda_{0i}$, $\lambda_{2i}$ are the zeroth and second moments of spectrum $S_{Ri}(n)$ about the frequency origin and are given as

$$\lambda_{m_i}=\int_0^\infty w^m S_{R_i}(n)dn \quad (32)$$

## NUMERICAL RESULTS

Using the procedure proposed in the previous sections, a computer programme was developed to evaluate the lateral-torsional response of typical tall building conforming to the dynamic characteristics discussed in the formulation of the equations of motion. The multi-storey building shown in Figure (2) is analyzed to conduct the parametric study. The following data are used:

Building and Foundation Data: The building has 10 stories of 4. 5m each or varied (i. e H=45m or varied), and plan dimensions B=15m and W$\geq$ B. A damping ratio $\zeta$=0. 05 is assigned for the first two modes. The geometric properties of the building are listed in Table (1). The eccentricity ratios $e_x/r$, $e_y/r$ for all floors are taken as 0. 2, 0. 3(respectively) or varied. The mass of footing $m_0$=67. 5 t. sec$^2$/m and the mass moments of inertia are $I_{0x}$=1265. 6 t. m. sec$^2$, $I_{0y}$=1265. 6 t. m. sec$^2$, $I_{0z}$=2531. 2 t. m. sec$^2$.
Soil Data: Mass density $\rho_s$=0. 18(t/m$^3$)/(m/sec$^2$), shear wave velocity $V_s$=70 m/sec or variable, shear modulus $G_s=V_s^2\rho_s$, and Poisson's ratio $\nu$=1/3.
Wind Data: The wind loading is represented by three components in along wind, across wind, and torsional directions at different floor levels. The matrix $[S_{fx}(n)]$ of PSDF of loads in along wind direction is obtained using Eqs. 2, 3 and 9-12 with shear velocity $U_*$=2. 2 m/sec., surface roughness height $Z_0$=0.07m, air density $\rho_a$=0.125 (kg/m$^3$)/(m/sec$^2$), drag coefficient $C_d$=1.2, and the decay constants $C_y$=16, $C_z$=10. The matrices $[S_{f\theta}(n)]$, and $[S_{fy}(n)]$ of the PSDF of across wind forces and torsional moments are obtained using Eqs. 13, 14 and Figure (1) and with the help of Eqs 11 and 12. The wind duration is taken as T=600 sec.

Table 1. Geometric properties of a 10-storey building.

| storey No.i | $m_i$ $t.s^2/m$ | $K_{xi}$ t/m | $K_{yi}$ t/m | $K_{\theta i}$ t.m/rad | $r_i$ m | $I_{xi}$ $t.m.s^2$ /rad | $I_{yi_2}$ $t.m.s^2$ /rad | $I_{zi}$ $t.m.s^2$ /rad |
|---|---|---|---|---|---|---|---|---|
| 1 | 22.5 | 35000 | 40000 | $2.8*10^6$ | 6.12 | 421.9 | 421.9 | 843.8 |
| 2 | 22.5 | 35000 | 40000 | $2.8*10^6$ | 6.12 | 421.9 | 421.9 | 843.8 |
| 3 | 22.5 | 35000 | 40000 | $2.8*10^6$ | 6.12 | 421.9 | 421.9 | 843.8 |
| 4 | 22.5 | 35000 | 40000 | $2.8*10^6$ | 6.12 | 421.9 | 421.9 | 843.8 |
| 5 | 15.0 | 23300 | 26600 | $1.9*10^6$ | 6.12 | 281.2 | 281.2 | 562.4 |
| 6 | 15.0 | 23300 | 26600 | $1.9*10^6$ | 6.12 | 281.2 | 281.2 | 562.4 |
| 7 | 15.0 | 23300 | 26600 | $1.9*10^6$ | 6.12 | 281.2 | 281.2 | 562.4 |
| 8 | 15.0 | 23300 | 26600 | $1.9*10^6$ | 6.12 | 281.2 | 281.2 | 562.4 |
| 9 | 11.2 | 17500 | 20000 | $1.4*10^6$ | 6.12 | 210.0 | 210.0 | 420.0 |
| 10 | 11.2 | 17500 | 20000 | $1.4*10^6$ | 6.12 | 210.0 | 210.0 | 420.0 |

The power spectra S(n) of top floor displacements and accelerations are shown in Figures (3) and (4), respectively. These for base shears and base moments are given in Figures (5) and (6), respectively. It can be seen that the most contribution to the response is limited in the low frequency range (n=.01-.8) except for torsional response this range may be extended up to n=1.7.

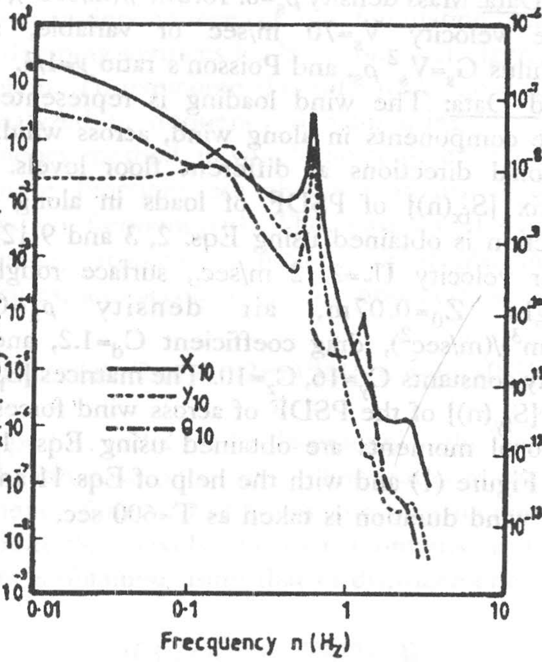


Figure 3. Power spectra of top floor displacements.

It is also seen that the variations of S(n) of the corresponding displacement, force, and moment (e. g $X_{10}$, $Q_{Bx}$, $M_{By}$) have similar trends. The distributions of the r. m. s values of shear forces $P_x$, $P_y$, and torsional moments $M_t$ at the different storey levels are shown in Figure (7). It is noted that higher forces are produced at the top floors due to the increase of wind velocity with the height .

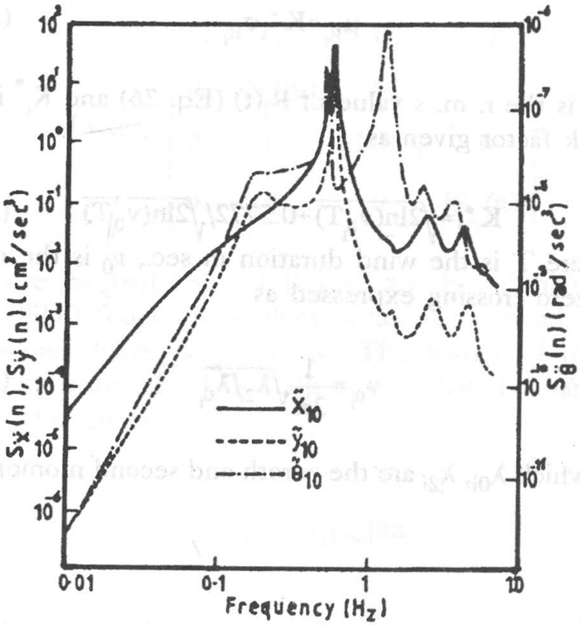


Figure 4. Power spectra of top floor accelerations.

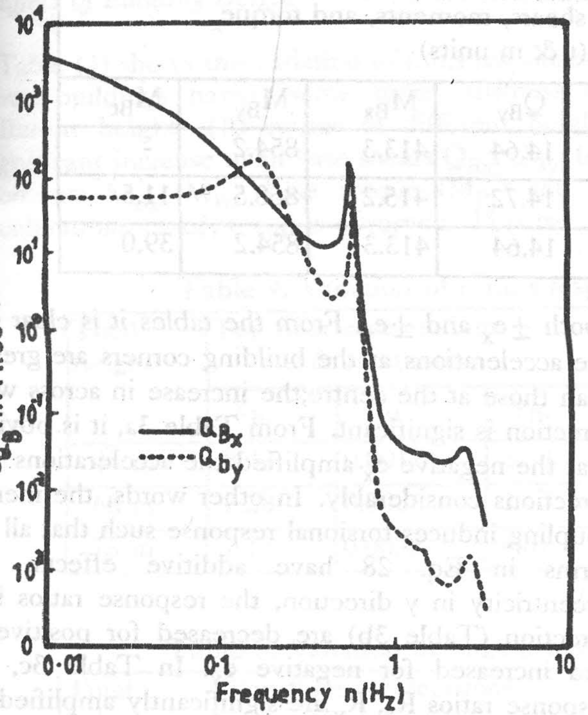


Figure 5. power spectra of base shears.

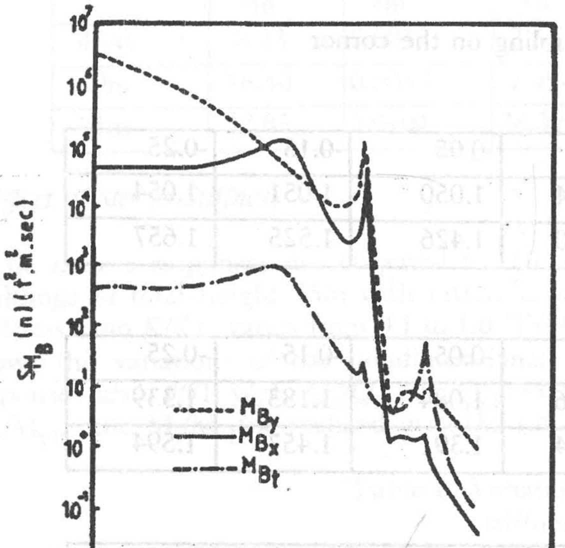


Figure 6. Power spectra of base moments.

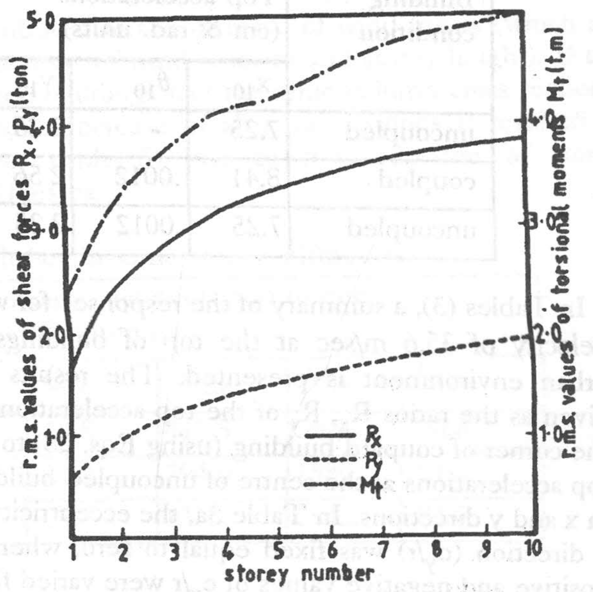


Figure 7. Distribution of storey forces $P_x$, $P_y$, $M_t$

*Effect of Torsional Coupling and Wind Induced Torsional Moments.*

In Table (2), a comparison is made between three conditions of 10 storey building. In the first two, the wind induced torsional moments are set equal to zero, whereas this effect is considered in the third case. The results of the first and third cases are obtained for uncoupled building (i. e $e_x/r= e_y/r=0.\ 0$), while the results in the second case are presented for torsionally coupled building ($e_x/r=0.\ 2$, $e_y/r=0.\ 3$). It can be noted that the torsional coupling produces significant values of torsional responses (rotation and moment), but, the increase of other response quantities is marginal. On the other hand, the wind induced torsional moments affect only the torsional responses. In general, the comparison of response levels in Table (2) emphasizes the importance of torsional response in the design of high rise building.

Table 2. Effect of torsional coupling and wind torsional moments.

| Building condition | Top accelerations (cm & rad. units) | | | Base shears, moments, and torque (t & m units) | | | | |
|---|---|---|---|---|---|---|---|---|
| | $x_{10}$ | $\theta_{10}$ | $y_{10}$ | $Q_{Bx}$ | $Q_{By}$ | $M_{Bx}$ | $M_{By}$ | $M_{Bt}$ |
| uncoupled | 7.25 | - | 2.25 | 31.4 | 14.64 | 413.3 | 854.2 | - |
| coupled | 8.41 | .0012 | 2.56 | 31.8 | 14.72 | 415.2 | 868.5 | 11.5 |
| uncoupled | 7.25 | .0012 | 2.25 | 31.4 | 14.64 | 413.3 | 854.2 | 39.0 |

In Tables (3), a summary of the responses for wind velocity of 35.6 m/sec at the top of buildings in urban environment is presented. The results are given as the ratios $R_x$, $R_y$ of the top accelerations at the corner of coupled building (using Eqs. 28) to the top accelerations at the centre of uncoupled building in x and y directions. In Table 3a, the eccentricity in y direction ($e_y/r$) was fixed equal to zero, whereas, positive and negative values of $e_x/r$ were varied from 0.0 to 0.25. In Table 3b, the eccentricity in x direction was set equal to zero, and positive and negative values of $e_y/r$ were varied from 0 to 0. 25. The results in Table 3c represent response ratios for both $\pm e_x$ and $\pm e_y$. From the tables it is clear that the accelerations at the building corners are greater than those at the centre;the increase in across wind direction is significant. From Table 3a, it is obvious that the negative $e_x$ amplified the accelerations in y directions considerably. In other words, the inertial coupling induces torsional response such that all the terms in Eq. 28 have additive effects. For eccentricity in y direction, the response ratios in x direction (Table 3b) are decreased for positive $e_y$ and increased for negative $e_y$. In Table 3c, the response ratios $R_x$, $R_y$ are significantly amplified for negative eccentricities.

Table 3. Effect of torsional coupling on the corner accelerations.

a-$e_y/r$=0.0

| $e_x/r$ | 0.0 | 0.05 | 0.15 | 0.25 | -0.05 | -0.15 | -0.25 |
|---|---|---|---|---|---|---|---|
| $R_x$ | 1.049 | 1.050 | 1.051 | 1.054 | 1.050 | 1.051 | 1.054 |
| $R_y$ | 1.383 | 1.345 | 1.279 | 1.230 | 1.426 | 1.525 | 1.657 |

b-$e_x/r$=0.0

| $e_y/r$ | 0.0 | 0.05 | 0.15 | 0.25 | -0.05 | -0.15 | -0.25 |
|---|---|---|---|---|---|---|---|
| $R_x$ | 1.049 | 1.024 | 0.996 | 0.996 | 1.084 | 1.183 | 1.339 |
| $R_y$ | 1.383 | 1.391 | 1.457 | 1.594 | 1.391 | 1.457 | 1.594 |

c-eccentricities in both directions

| $e_y/r$ $e_x/r$ | 0.0 | 0.05 | 0.15 | 0.25 | -0.05 | -0.15 | -0.25 |
|---|---|---|---|---|---|---|---|
| $R_x$ | 1.049 | 1.024 | 0.995 | 0.985 | 1.084 | 1.190 | 1.377 |
| $R_y$ | 1.383 | 1.352 | 1.336 | 1.377 | 1.435 | 1.630 | 2.080 |

*Effect of Building Height*

Table (4) shows the variation of r.m.s responses of three buildings having same storey stiffness and different heights (10 stories of different heights) Significant increase of all base shears $Q_{Bx}$, $Q_{By}$, base moments $M_{Bx}$, $M_{By}$, base torque ($M_{Bt}$) and top accelerations (except $x_{10}$) is observed. This is attributed to the increase of wind forces (which are functions of wind velocity and storey height). If the three buildings had the same column cross sections, further increase of all r. m. s values is resulted in (see Table 5) due to the reduction of storey stiffnesses.

Table 4. Variation of r. m. s responses with height-same storey stiffnesses.

| Total height | Top floor accelerations (cm & rad units) | | | Base shears, moments and torque (t & m units) | | | | |
|---|---|---|---|---|---|---|---|---|
| | $x_{10}$ | $\theta_{10}$ | $y_{10}$ | $Q_{Bx}$ | $Q_{By}$ | $M_{Bx}$ | $M_{By}$ | $M_{Bt}$ |
| 45 m | 8.43 | 0.0017 | 2.58 | 31.9 | 14.8 | 415.5 | 869 | 40.8 |
| 60 m | 7.28 | 0.0026 | 3.47 | 44.1 | 21.2 | 794.0 | 1589 | 61.2 |
| 75 m | 7.18 | 0.0036 | 4.67 | 56.9 | 29.0 | 1353. | 2542 | 83.0 |

Table 5. Variation of r.m.s responses with height-same column cross section.

| Total height | Top floor accelerations (cm & rad units) | | | Base shears, moments and torque (t & m units) | | | | |
|---|---|---|---|---|---|---|---|---|
| | $x_{10}$ | $\theta_{10}$ | $y_{10}$ | $Q_{Bx}$ | $Q_{By}$ | $M_{Bx}$ | $M_{By}$ | $M_{Bt}$ |
| 45m | 8.43 | 0.0017 | 2.58 | 31.9 | 14.8 | 415.5 | 869 | 40.8 |
| 60m | 16.40 | 0.0050 | 7.49 | 46.4 | 22.8 | 855.0 | 1677 | 68.2 |
| 75m | 32.85 | 0.0104 | 28.39 | 63.3 | 42.5 | 1996 | 2860 | 101.6 |

*Effect of Storey Stiffness*

The r. m. s responses are obtained for 10 storey buildings of total height 45m with different storey stiffness ratio K/K1 (varies from 0.1 to 1.0. Table (6) shows the variations of the nondimensional r.m.s responses x/x1, $\theta/\theta 1$, y/y1, $Q_x/Q_{x1}$, $Q_y/Q_{y1}$, $M_x/M_{x1}$, $M_y/M_{y1}$, and $M_t/M_{t1}$(normalized w.r.t the r.m.s responses obtained at stiffness ratio K/K1=1.0) with the stiffness ratio K/K1. From the table it can be noted that as K/K1 decreases from 1.0 to 0.1, the top floor accelerations are increased significantly (3.3-7.3 times);however, the increase of base forces is not that much (1.3-1.8 times). It can be seen also that the increase of the responses in the across wind and rotational directions is pronounced.

Table 6. Variation of r.m.s responses with storey stiffness-same total height.

| Stiffness ratio K/K1 | Normalized accelerations | | | Normalized base shears, moments,and torque | | | | |
|---|---|---|---|---|---|---|---|---|
| | x/x1 | $\theta/\theta 1$ | y/y1 | $Q_x/Q_{x1}$ | $Q_y/Q_{y1}$ | $M_x/M_{x1}$ | $M_y/M_{y1}$ | $M_t/M_t$ |
| 1.00 | 1.00 | 1.00 | 1.00 | 1.00 | 1.00 | 1.00 | 1.00 | 1.00 |
| 0.50 | 1.35 | 1.64 | 2.72 | 1.03 | 1.10 | 1.10 | 1.03 | 1.06 |
| 0.25 | 2.04 | 3.28 | 4.25 | 1.10 | 1.26 | 1.26 | 1.11 | 1.26 |
| 0.10 | 3.28 | 7.35 | 7.07 | 1.30 | 1.68 | 1.68 | 1.32 | 1.80 |

*Effect of Soil Flexibility*

The effect of the soil-structure interaction depends on the soil condition (represented by the shear wave velocity $V_s$). The variation of the r.m.s responses with $V_s$ is given in Table 7, in which the r.m.s responses of the fixed base building (no interaction takes place) are also given. From the table it is clear that the top displacements are reduced for higher values of $V_s$, ultimately ($V_s$=300 m/sec) reaching those for fixed base building. The base forces increase with $V_s$ up to certain value $V_s$=150 m/sec (representative to medium soil) then they decrease slightly up to $V_s$=300 m/sec, after which they attain stationary values that are identical to those of fixed base building. In general, the interaction effects are pronounced for low values of $V_s$(e. g $V_s$=30 m/sec) representing very soft soil where the displacements in x and y directions are increased by 75% and 133%, respectively; while the base forces are decreased by 3-5%. However, the effect of soil flexibility on the base torque is insignificant.

Table 7. Effect of soil flexibility on r.m.s responses

| $V_s$ m/sec | Top floor displacements (cm & rad units) | | | Base shears and moments (t & m units) | | | | |
|---|---|---|---|---|---|---|---|---|
| | $x_{10}$ | $\theta_{10}$ | $y_{10}$ | $Q_{Bx}$ | $Q_{By}$ | $M_{Bx}$ | $M_{By}$ | $M_{Bt}$ |
| 30 | 1.26 | .000228 | 0.70 | 30.70 | 14.5 | 409.0 | 835.0 | 44.1 |
| 70 | 0.96 | .000219 | 0.37 | 31.90 | 14.8 | 415.5 | 869.0 | 40.8 |
| 100 | 0.82 | .000220 | 0.34 | 32.00 | 14.8 | 419.0 | 873.0 | 39.8 |
| 150 | 0.77 | .000227 | 0.32 | 32.40 | 14.9 | 421.0 | 884.0 | 40.5 |
| 200 | 0.75 | .000225 | 0.31 | 32.30 | 14.9 | 421.0 | 881.0 | 39.9 |
| 300 | 0.73 | .000223 | 0.30 | 32.19 | 14.9 | 420.5 | 877.6 | 39.4 |
| 450 | 0.72 | .000222 | 0.30 | 32.17 | 14.9 | 419.8 | 877.0 | 39.2 |
| 600 | 0.72 | .000221 | 0.30 | 32.16 | 14.9 | 419.0 | 876.5 | 39.0 |
| fixed base | 0.72 | .000220 | 0.30 | 32.13 | 14.83 | 418.5 | 875.6 | 38.8 |

The r.m.s values of the base forces shown in Table (7) are calculated at the lower ends of the ground floor columns i.e the forces acting at the foundation level are not included. The r.m.s forces are calculated again at the foundation level for different values of $V_s$. Table 8 shows the variations of these forces (normalized w.r.t those obtained for $V_s$=600 m/sec) with $V_s$. As $V_s$ decreases from 600 m/sec (representing extremely firm soil) to 30 m/sec (representative of very soft soil), the base shears and moments are reduced by 7-13%; nevertheless the base torque is reduced significantly (a reduction of 41% is observed).

The comparison between Tables (7) and (8) shows that the effect of soil flexibility on the storey forces is marginal. This can be explained from the following observation:

The dominant energy of the wind induced forces is confined only within a low frequency range (see Figure (1)) and the storey forces are produced mainly in higher modes having natural frequencies greater than this range. Thus, there is no dynamic amplification of the response i. e the system responds in a pseudo static manner(see Figure (8)). For more flexible soil, the natural frequencies are reduced (due to the reduction of soil stiffness) but still they are higher than the frequencies over which the dominant energy of the wind induced forces is confined. As a result the system again behaves pseudo statically (see Figure (9).

Table 8. Effect of soil flexibility on the r. m. s shears and moments at the foundation level.

| $V_s$ m/sec | Normalized r.m.s values of shears and moments at the foundation level | | | | |
|---|---|---|---|---|---|
| | $Q_{Bx}$ | $Q_{By}$ | $M_{Bx}$ | $M_{By}$ | $M_{Bt}$ |
| 30 | 0.873 | 0.936 | 0.943 | 0.870 | 0.588 |
| 70 | 0.975 | 0.968 | 0.972 | 0.982 | 0.645 |
| 100 | 0.992 | 0.994 | 0.998 | 0.998 | 0.708 |
| 200 | 1.018 | 1.022 | 1.023 | 1.022 | 0.962 |
| 300 | 1.006 | 1.012 | 1.012 | 1.006 | 0.986 |
| 450 | 1.003 | 1.004 | 1.004 | 1.004 | 1.005 |
| 600 | 1.000 | 1.000 | 1.000 | 1.000 | 1.000 |

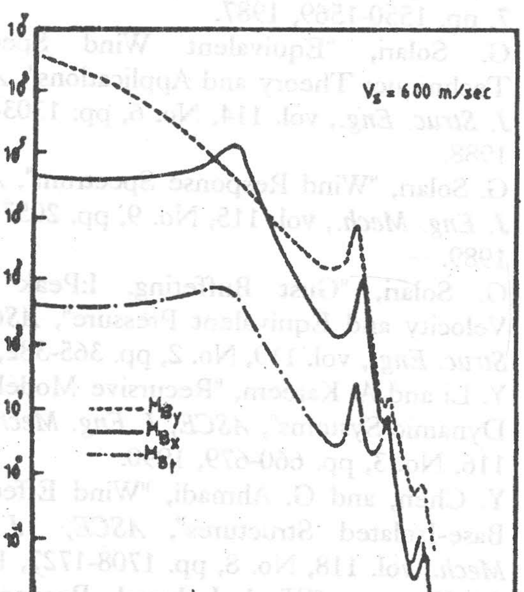


Figure 8. Power spectra of base moments.

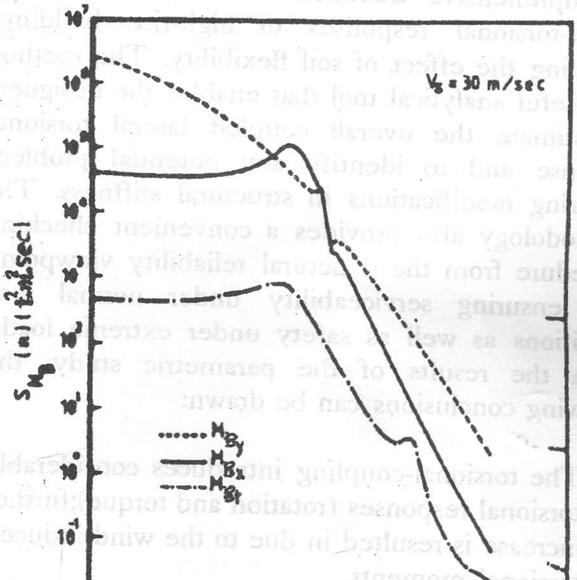


Figure 9. Power spectra of base moments.

*Peak Responses*

The peak factors $K^*$ obtained, (using Eq. 30) for soft soil condition ($V_s$=70m/ sec) are 3.38 for $Q_{Bx}$, $M_{By}$; 3.34 for $Q_{By}$, $M_{Bx}$); 3.62 for base torque ($M_{Bt}$); and range between 3.44, 3.48 for top the floor displacements and 3.59, 3.60 for the top floor accelerations. The peak factors increase with the increase of $V_s$. As $V_s$ is increased from 30 m/sec (very soft soil) to 600 m/sec (extremely firm soil), the peak factors are increased from 3.12 to 3.54 for $Q_{Bx}$, $M_{By}$; from 3.25 to 3.52 for $Q_{By}$, $M_{Bx}$; and from 3.51 to 3.72 for $M_{Bt}$. This trend magnifies the effect of soil flexibility on the base forces.

CONCLUSION

The methodology presented in this paper provides a comprehensive treatment of the wind induced lateral-torsional responses of high-rise buildings including the effect of soil flexibility. The method is a useful analytical tool that enables the designers to estimate the overall coupled lateral torsional response and to identify any potential problem requiring modifications in structural stiffness. The methodology also provides a convenient checking procedure from the structural reliability viewpoint, thus ensuring serviceability under normal load conditions as well as safety under extreme loads. From the results of the parametric study, the following conclusions can be drawn:

(i) The torsional-coupling introduces considerable torsional responses (rotation and torque);further increase is resulted in due to the wind induced torsional moments.

(ii) The corners of a building experience considerable effect of torsional response e. g excessive human discomfort (expressed by top accelerations). The top corner accelerations are affected much by the magnitude and direction of building eccentricities

(iii) The wind effect (represented by the top floor accelerations and base forces) increases significantly with the height. This trend is pronounced for flexible buildings and those having aspect ratio H/B ≥ 4.

(iv) The increase of base flexibility (very soft soil) magnifies the horizontal displacements of the structure considerably (75-133% greater than those obtained for firm soil) due to the rigid body motion of the soil-structure system. On the other hand, the shears and moments at the foundation level are reduced about 7-13% and the torque moment is reduced by 41% for very soft soil. The amplifications and deamplifications are enhanced due to the increase of peak factors with the soil flexibility.

REFERENCES


[1] A. G. Davenport, "Gust Loading Factors", *ASCE, J. Struc. Eng.* vol. 93, No. 3, pp. 11-34, 1967.

[2] J. Vellozzi and E. Cohen, "Gust Response Factors", *ASCE, J. Struc. Eng.*, vol. 94, No. 6, pp. 1295-1313, 1968.

[3] G. Solari, "Turbulence Modeling for Gust Loading", *ASCE, J. Struc. Eng.*, vol. 113, No. 7, pp. 1550-1569, 1987.

[4] G. Solari, "Equivalent Wind Spectrum Technique: Theory and Applications", *ASCE, J. Struc. Eng.*, vol. 114, No. 6, pp. 1303-1323, 1988.

[5] G. Solari, "Wind Response Spectrum", *ASCE, J. Eng. Mech.*, vol. 115, No. 9, pp. 2057-2072, 1989.

[6] G. Solari, "Gust Buffeting. I:Peak Wind Velocity and Equivalent Pressure", *ASCE, J. Struc. Eng.*, vol. 119, No. 2, pp. 365-382, 1993.

[7] Y. Li and A. Kareem, "Recursive Modeling of Dynamic Systems", *ASCE, J. Eng. Mech.*, vol. 116, No. 3, pp. 660-679, 1990.

[8] Y. Chen, and G. Ahmadi, "Wind Effects on Base-Isolated Structures", *ASCE, J. Eng. Mech.*, vol. 118, No. 8, pp. 1708-1727, 1992.

[9] A. Kareem, "Wind Induced Response of Buildings", *Proc. Int. Conf. Wind Loads on Structures*, New Delhi, India, pp. 67-88, 1990.

[10] M. S. Islam, B. Ellingwood, and R. B. Corotis, "Dynamic Response of Tall Buildings to Stocastic Wind Load", *ASCE, J. Struc. Eng.*, vol. 116, No. 11, pp. 2982-3002, 1990.

[11] M. S. Islam, B. Ellingwood, and R. B. Corotis, "Wind-Induced Response of Structurally Asymmetric High-Rise Buildings.", *ASCE, J. Struc. Eng.*, vol. 118, No. 1, pp. 207-222, 1992.

[12] A. Kareem, J. E Cermak, and J. A Peterka, "Crosswind Response of High-Rise Buildings", *Proc. 5th Int. Conf. on Wind Eng.*, VI-1, pp. 1-14, Colorado, U.S.A, 1979.

[13] K.C Kwok, and W.H Melbourne, "Cross-Wind Response of Structures Due to Displacement Dependent Lock-in Excitation", *Proc. 5th Int. Conf. Wind Eng.*, VI-4, pp. 1-10, Colorado, U. S. A, 1979.

[14] H. Tsukagoshi, Y. Tamura, A. Sasaki, and H. Kanai, "Response Analyses on Along-Wind and Across-Wind Vibrations of Tall Buildings in Time Domain" *J. Wind Eng. and Indust. Aerodyn.* vol. 36, pp. 497-507, 1993.

[15] J. F. Sidarous, and M. D. Vanderbilt, "An Analytical Methodology for Predicting Dynamic Building Response to Wind", *Proc. 5th Int. Conf. Wind Eng.*, VI-5, pp. 1-15, Colorado, U. S. A, 1979.

[16] A. Kareem, "Lateral-Torsional Motion of Tall Buildings to Wind Loads", *ASCE, J. Struc. Eng.*, vol. 111, No. 11, pp. 2479-2496, 1985.

[17] C. Solari, and D. Stura, "Dynamic Alongwind Response of a Structural System Including Soil Flexibility", *Proc. 5th Int. Conf. Wind Eng.*, VI-7, pp. 1-11, Colorado, U.S.A, 1979.

[18] A. Pais and E. Kausel, "Approximate Formulas for Dynamic Stiffnesses of Rigid Foundations", *J. Soil Dyn. & Earthqu. Eng.* vol. 7, No. 4, pp. 213-227, 1988.